Tridimensional morphology and kinetics of etch pit on the {0001} plane of sapphire crystal

Lunyong Zhang[*,1], Hongbo Zuo[2], Zhiyong Yuan[2], Ji Zhou[1], Jianfei Sun[,1], Dawei Xing[1], Jiecai Han[2]**

[1] School of Materials Science and Engineering, Harbin Institute of Technology, Harbin, P.R.China, 150001
[2] Center for Composite Materials, Harbin Institute of Technology, Harbin, P.R.China, 150001

Keywords Sapphire crystal; Etch pit; Tridimensional morphology; Etching kinetics; Structure origin; Kinematic wave

[*] Corresponding author: e-mail jfsun_hit@263.net, Phone: +86 451 6418317
[**] e-mail allen.zhang.ly@gmail.com

The tridimensional morphology and etching kinetics of the etch pit on the C-{0001} plane of sapphire crystal (α-Al_2O_3) in KOH molten were studied experimentally. It was shown that the etch pit takes on tridimensional morphologies with triangular symmetry same as the symmetric property of the sapphire crystal. Pits like centric and eccentric triangular pyramid as well as hexagonal pyramid could be observed, but the latter is much less in density. Analyses show the side walls of the etch pits belong to the $\{1\bar{1}0\bar{2}\}$ family, and the triangular pit contains edges full composed by Al^{3+} ions on the etching surface so it is more stable than the hexagonal pit since whose edges on the etch surface contains Al^{2+} ions. The etch pits developed in manner of kinematic wave by the step moving with constant speed controlled by the chemical reaction with activation energy of 96.6KJ/mol between Al_2O_3 and KOH.

1 Introduction Sapphire single crystal combines many good mechanical and optical properties that make it has played an increasingly significant role in engineering and science since the twentieth century [1, 2]. Today, Sapphire has been applied in the following field: substrates for light-emitting diodes, projectors, microwave devices, windows for civilian and military equipment, *et al.* [2]. However, crystalline defects like dislocation, stack fault would intensely worsen the properties of sapphire. Thus, the characterization of crystalline defects is becoming increasingly important [3], leading to the renaissance of wet etch method.

Wet etch is the simplest method to date for elucidating the surface defects and the structure symmetry of crystal[4]. Its principle is that every crystalline solid in contact with proper corrosive liquid etchants undergoes decrystallization which always begins at the most active points on the surface, such as the places where dislocations reach surface[5, 6]. When the decrystallization along surface is slower than that along the direction perpendicular to surface, etch pit can be observed [5]. Always, the shape of crossover section between etching surface and defect determines that etch pit corresponding is spotted state or linear state[7], and the symmetry of structure of etching surface determines the symmetry of etch pit. Thus, the density of defect can be obtained by counting the etch pits, the type of defect can be analyzed by the state of etch pit, the structure symmetry of crystal can be analyzed by the symmetry of etch pit.

In the past several decades, wet etch and etch pits of sapphire have been studied by some scientists. They pointed out that only a few etchants can be used to develop pits at dislocation sits under high temperature for the high resistance of sapphire to chemical attack [3]. Those etchants are phosphoric acid (H_3PO_4)[8] , potassium bisulfate ($KHSO_4$) [9], borax ($Na_2B_4O_7$) [3, 10], potassium hydroxide (KOH) [10] and 15%HCl+15%HNO_3+H_2O [1]. KOH maybe the most popular for it can almost etch all the main crystallographic faces of sapphire. Up to now, triangular[1, 3, 7, 10], hexagonal[1, 3, 7] and quadrilateral[1] etch pits have been observed on *c*-plane {0001} of sapphire. On *a*-plane $\{11\bar{2}0\}$, only rhombic pyramidal etch pits were observed [3, 9]. On plane $\{10\bar{1}1\}$, the etch pits are triangular or rhombic, and hexagonal on plane {1100} [7]. However, these results just shown the projection shape of the etch pit on the etched surface, the tridimensional morphology, so the information coming from the inside of

etch pit with which the formation of etch pit could be studied more intensively, is deficiency.

In the present work, the etch pit of dislocation on the c-{0001} plane of sapphire crystal was developed using KOH molten and then the tridimensional morphology of etch pit was characterized by optical microscopy and laser scanning confocal microscopy. Moreover, the etch kinetics of etch pit was studied.

2 Experimental Sapphire crystals were grown by the sapphire growth technique with micro-pulling and shoulder-expanding at cooled centre (SAPMAC)[11] using high purity Al_2O_3 powders (5N). cubic specimens covered with *c*-plane (0001), *a*-plane ($11\bar{2}0$) and *m*-plane ($1\bar{1}00$) were cut from a sapphire crystal about Ø200×250mm (the specimen for revealing the etch pit morphology was cut from the region containing tiny bubbles, the specimens for studying the kinetics of etch pit were cut from optical grade region), and then all the planes were polished to optical grade, namely surface roughness is smaller than Rz0.01 and plane misorientation is smaller than 3°, through chemo-mechanical process with low distribution Ø40nm-SiO_2 based slurry of PH=11.7 at temperature of 40℃ and pressure of 0.15MPa. The chemical etch was performed in KOH molten in an Al_2O_3 crucible. The etch temperatures were 320℃ for revealing the morphology of etch pit, and 280℃, 300℃ and 310℃, respectively, for studying the kinetics of etch pit. While etch, KOH powders (99%) and the specimen were separately put in a furnace with temperature error ≤1℃ and then heated to the etch temperature together, then the specimen was put into the KOH molten rapidly and keeping the etch temperature for a desired duration, then the specimen was taken out from the KOH molten and naturally cooled in the furnace. Next, the specimen was treated in dilute HCl (≈0.5%) and in boiling water to remove the residual KOH and any remaining surface film [10], then washed in distilled water for 30min and desiccated by a blow-dryer. The etch pit was observed by means of NOVEl NJF-120A optical microscopy and by OLYMPUS 3100 laser scanning confocal microscopy (LSCM).

The etch duration was larger than 30 min for revealing the etch pit morphology. During the experiment for studying etch kinetics, the specimen was firstly etched for 5min following by etch pit morphology observation, and then the same specimen was etched repeatedly for 2min in fresh KOH molten, and the etch pit morphology was observed after every etch.

3 Results and discussions

3.1 Etch pit morphology Ref [1] stated that etch pit on the C-{0001} plane of sapphire crystal can bear cross section with quadrilateral shape besides triangular shape and hexagonal shape. In our experiment, only etch pits with triangular shape and hexagonal shape cross section were observed, as shown in Fig.1. It is indicated that the cross section of triangular etch pit is an equilateral triangular with edges along directions $[11\bar{2}0]$, $[\bar{2}110]$ and $[1\bar{2}10]$. The hexagonal etch pit shown a cross section with three groups of parallel edges along directions $[11\bar{2}0]$, $[\bar{2}110]$ and $[1\bar{2}10]$, the lengths of two edges in every group are different, but the lengths of the long edges as well as the lengths of the short edges are equal. These observations are consistent with the results obtained by Liu *et al*.[3].

Further on, the tridimensional morphology of the etch pits were displayed. Most of the triangular etch pits are perpendicular pyramid (dotted arrow points in Fig.1a) and perpendicular pyramid frustum (solid arrow points in Fig.1a), and several of them are oblique pyramid shaped pit (dash dotted arrow points in Fig.1a). Besides, no kinks on the sidewalls of the etch pits are observed. For the hexagonal etch pit, just shallow pyramid frustum was found.

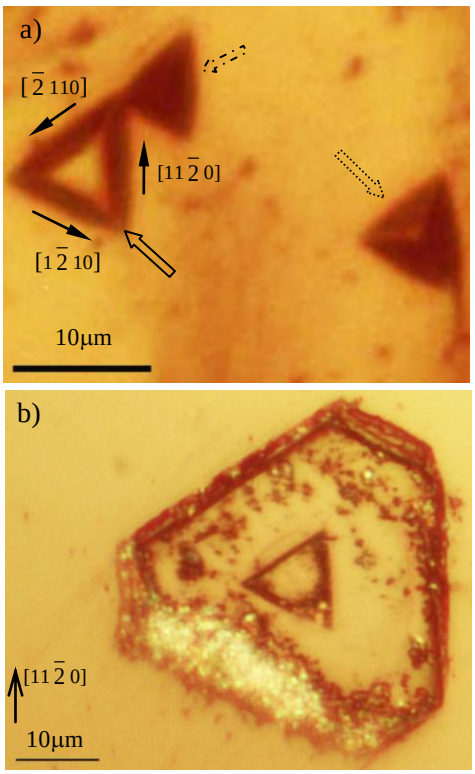

Figure 1 Morphologies of dislocation etch pits on the C-{0001} plane of sapphire crystal.

Motzer and Reichling [12] have classified the etch pit with perpendicular tridimensional morphology as centric pit independent of their appearance as pointed or flat bottomed, and stated that centric pit is solely a result of localized subsurface defects such as, in speculation, single impurities, impurity clusters and small dislocation loops or vacancy clusters but not of dislocations terminating at the surface which was contrarily attributed to the defect source of eccentric etch pit, *i.e.* the oblique pyramid shaped etch pit, especially where the dislocation line is believed to be incline to the etched surface. However, classical views believe that centric etch pit is associated with dislocation line perpendicular to the etching surface [13-15]. Considering

the specimen here for revealing etch pit morphology was cut from the region containing bubble defects and the dislocation line easiest formed in sapphire crystal lies in {0001} plane since the basal slip system of sapphire crystal is {0001}1/3[11$\bar{2}$0⟩ [16], we conjecture the centric etch pits observed by us is caused by localized subsurface defects including nano-bubbles and vacancy clusters, at the same time, we do not exclude the possibility that some of the centric etch pits were related with dislocations because sapphire crystal has weak slip systems {$\bar{1}$2$\bar{1}$0}[10$\bar{1}$0⟩[16], {10$\bar{1}$0}[11$\bar{2}$0⟩ and {11$\bar{2}$0}[10$\bar{1}$0⟩[6] associated with which the dislocation line is perpendicular to the {0001} plane.

Ref [12] has called the frustum shaped etch pit as flat bottomed etch pit and states that it is a consequence of the removing of localized subsurface defects from crystal, implying that the bottom structure of etch pit is independent on the crystal structure and the etching conditions and it is reasonable to argue that the point bottomed etch pit and the flat bottomed etch pit are same from the point of view of indicating the crystal structure and etching conditions. Therefore, the tridimensional morphologies of the etch pits on the {0001} plane of sapphire crystal are regular triangular pyramid and hexagonal pyramid with triangular symmetry.

3.2 Crystal structure origin of etch pit morphologies It has been shown that the etch pit morphologies possible formed on the C-{0001} plane of sapphire crystal are triangular symmetry, generally corresponding to the $R\bar{3}C$ symmetry of the lattice structure of sapphire crystal [6]. At atomic scale, the edges of a etch pit on the etching surface were regarded to be composed by the oxygen atoms in directions [11$\bar{2}$0], [$\bar{2}$110] and [1$\bar{2}$10][3]. In our opinion, the C-{0001} plane of sapphire crystal could be classified into two kinds of planes, namely oxygen atomic plane and aluminium atomic plane since sapphire crystal, according to its crystal structure[17], is composed by aluminium layer and oxygen layer alternately and the aluminium layers as well as the oxygen layers have same topological structure in atomic configuration, and the edges of etch pits on the {0001} etching surface should be composed by the aluminium atoms since the aluminium ion is more stable in chemistry than the oxygen ion. From the view of their bond character, every Al^{3+} ion bonds with three O^{2-} ions and every O^{2-} ion bonds with two Al^{3+} ions, leading that an Al^{3+} ion still bonds with two O^{2-} ions after losing an Al-O bonding, however, it just leaves one Al-O bonding for an O^{2-} ion. Theoretical calculations have shown that the energies necessary for removing an Al^{3+} ion and an O^{2-} ion from sapphire crystal matrix are 9.1ev and 3.5ev, respectively[18], and the termination by a single Al layer has the lowest energy among the possible {0001} surfaces [19-21].

Fig.2 gives out the morphology and corresponding atomic configuration of the fringe of a etch pit on an aluminium atomic {0001} plane of sapphire crystal, which indicating that removing an Al^{3+} ion would cause the three oxygen atoms bonding with the Al^{3+} ion to become single bond ion which can be removed in the following etch, leaving behind three aluminium atoms with two bonds in the bottom layer, a relatively high stable state of aluminium atom in sapphire crystal, so the O^{2-} ions bonding with them can be kept, correspondingly the six aluminium atoms adjacent to the removed Al^{3+} ion in the top layer can be kept and formed the regular triangular shaped fringe with three edges in directions [11$\bar{2}$0], [$\bar{2}$110] and [1$\bar{2}$10] of the etch pit shown in section 3.1.

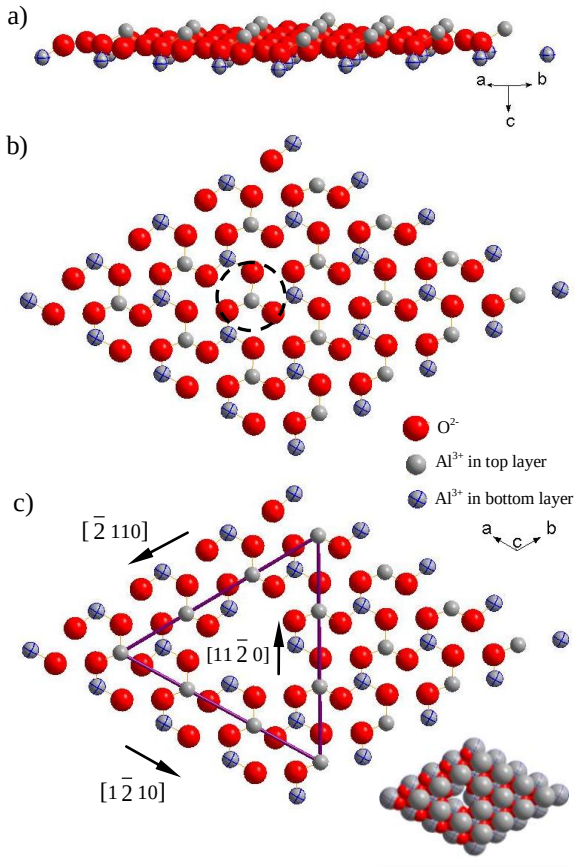

Figure 2 Schematic showing c) the atomic configuration of a triangular pit formed by removing an [AlO_3] group (looped by dashed circle) from the aluminium atomic C-{0001} plane, where the atomic configuration projected in a) [11$\bar{2}$0] direction, in b) [000$\bar{1}$] direction of the corresponding perfect crystal matrix. (crystal structure data coming from Ref[17])

Fig.1b demonstrates that the short edges of the hexagonal pit lies at the location original occupied by the angles of the triangular pit, indicating the short edges is a result of the un-full development of the angles. Fig.3 gives out the atomic configuration for the hexagonal pit. Because several sub-stable aluminum atoms with two Al-O bonds do not removed for possible reason, three short edges could be formed at the angle locations. With regard to the

reason causing the Al^{2+} ions not being removed, existing references believed that impurities play a significant role, especially they are more possibly absorbed by kinks [14] so depress the atom removing at kinks. As a consequence, the edges composed by the atom at kinks can develop. In Fig.3, the Al^{2+} ions not being removed nicely locate at the kinks site so the short edges could be formed under the impact coming from impurities.

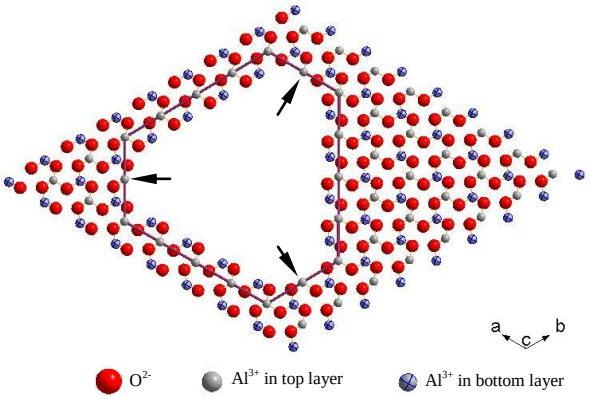

Figure 3 Atomic configuration of the hexagonal pit on the C-{0001} plane of sapphire crystal, where arrows indicate the Al^{2+} ions still staying in the top layer

In deed, here we depicted two relatively high sub-stable atomic configurations under etching damage for a C-{0001} plane of sapphire crystal. The configuration of the triangular pit is stronger than that of the hexagonal pit in stability due to the latter contains Al^{2+} ions in the etching surface. Form the point of view of the periodic bond chain theory (PBC theory)[22] and general energy opinion, the closed arrangement direction of atoms is lowest in energy and corresponds to the PBC direction which is considered as the most stable crystal direction in which the edges of the most stable etch pit should lies [14]. In Fig.2 and Fig.3, all of the etch pit edges are along the most closed arrangement directions $[11\bar{2}0]$, $[\bar{2}110]$ and $[1\bar{2}10]$, the atomic configurations are high sub-stable. However, the configuration of the hexagonal pit is less stable than that of the triangular pit owing to the Al-O bonds composing the short edges have become weaker for containing Al^{2+} ions.

In practice, the etch pit will ceaselessly grow by the atomic removing of the etchant. We just can observe the atomic configuration with longest living time, which right is the basic principle of the Monte Carlo simulation of etch pit morphology[23]. Obviously, the more stable triangular configuration would have longer living time than the hexagonal configuration, in that the triangular etch pit should be observed more, this has been indicated in the etch morphology revealing experiment.

In the above idea, we believed that three oxygen atoms would easily be removed when the aluminium atom bonding with them is removed by etchant, after that a relatively stable atomic configuration forms, implying the etching of sapphire crystal could be deemed as a chemical course accomplished by the removing of group $[AlO_3]$. Actually, the Ab initio study has shown that the $[AlO_3]$ group plays a great role in the interaction of water with the aluminium terminated {0001} sapphire crystal surface[24].

According to the relatively stablest atomic configuration of etch pit shown in Fig.2, a conclusion can be drawn that the side walls of the etch pit should go through the Al^{3+} ions and Al^{2+} ions adjacent to the removed $[AlO_3]$ group, as shown in Fig.4. These planes belong to the $\{1\bar{1}0\bar{2}\}$ family based on the crystal structure of sapphire and the angles between them and the {0001} plane are 57.6°, which is consistent with the measurement result in the etch kinetics experiments shown in the following section 3.3.

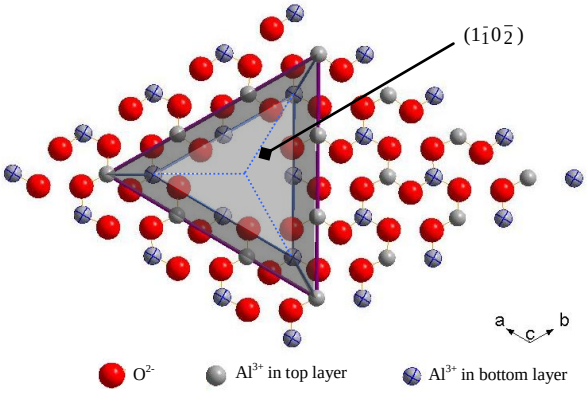

Figure 4 Schematic showing the atomic configuration of the predicted side walls of regular triangular pyramid shaped etch pit on the C-{0001} plane of sapphire crystal.

3.3 Kinetics of etch pit development Fig.5 lists the morphologies (observed by LSCM) of a etch pit undergoing different etch durations in 280℃ KOH molten, where the etch pit morphologies before 15min were not shown since they were too small to be detected clearly and the contrast and brightness of some images have been adjusted generally. Generally, the etch pit kept a morphology between the regular triangular pyramid and the hexagonal pyramid. Fig.6 exhibits the vertical sections of the etch pit at different durations, showing that the etch pit is flat bottomed and the side wall was flat plane during the etching. Further measurements of the angle of the right side wall with respect to the flat bottom paralleling to the {0001} etching surface illustrated the angle varied little around an average value 57.2° (Fig.7) which agreed with the angle $(0001)\wedge(1\bar{1}0\bar{2})$ mentioned in section 3.2, indicating the side walls of regular triangular pyramid shaped etch pit certainly belong to the $\{1\bar{1}0\bar{2}\}$ family, a relatively closed packed crystal plane of sapphire crystal.

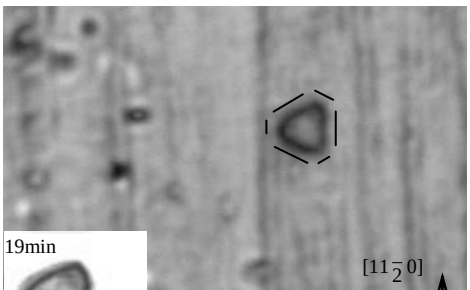

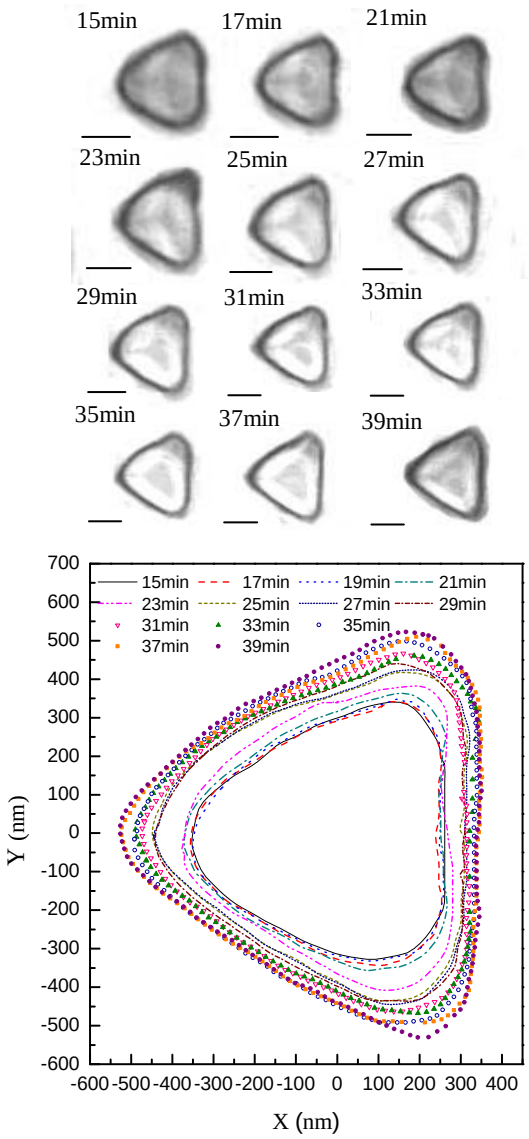

Figure 5 Etch pit morphologies developed in 280℃ KOH molten after different etch durations (scale bars not indicated represent 400nm).

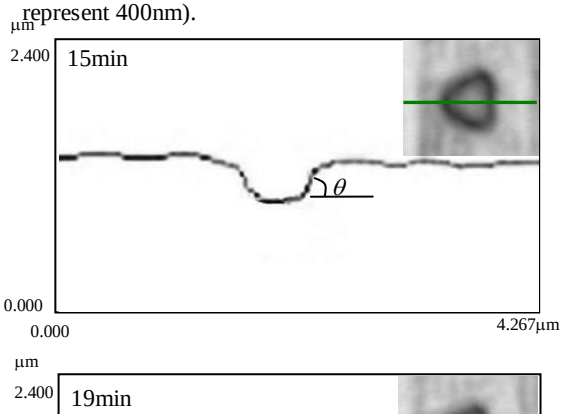

Figure 6 Etch pit morphologies after different etch durations

The inclining angle of the side walls did not change during the etching, on the other hand, implies that the etch was accomplished through the travel of step in kinematic wave[14]. In the context of kinematic theory of etching, a schematic showing the etch pit development was plotted as Fig.8, where v_m represents etching speed of the etching surface, v_D is the measured travelling speed of the pit edge, v_s indicates the travelling speed of the steps. Δt is the etching duration between two times of measurements and γ is the inclining angle of the spatial trace of the pit edge with respect to the etching surface. A relation among v_m, v_D and v_s thus can be derived as following

$$v_s = v_m\left(\cot\theta + \cot\gamma\right) = v_D\left(1 + \tan\gamma\cot\theta\right) \qquad (1)$$

Fig.9 gives out the distances of the edges with respect to the gravity centre (considered as a fixed point) of the etch pit. It can be seen that the distances nearly bear linear relations with etch duration, means the edges taken on constant travelling speeds which are 7.74nm/min and 3.97nm/min respectively for the short edges and the long edges on average. As a result, the spatial trace of the pit edge should be a line (γ=constant); the travelling speeds of the steps were constant; the etching speed of the etching surface was a constant.

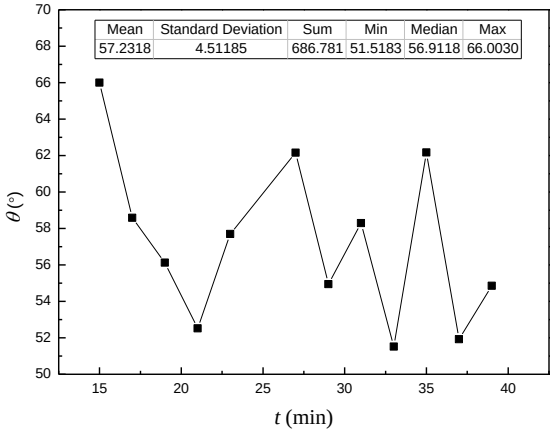

Figure 7 Inclining Angle of the right side wall with respect to the {0001} etch surface.

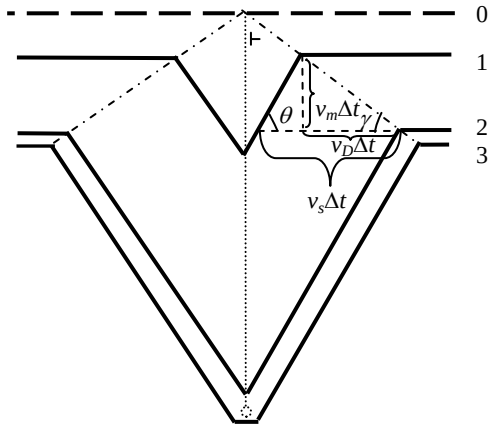

Figure 8 Kinematic wave development of the etch pit.

According to Refs [25] and [26], the step travelling speed of dislocation etching takes a Arrhenius relationship with etch temperature. That is

$$v_s = A\exp(-\frac{\Delta E}{KT}) \quad (2)$$

Where A is a frequency factor independent on the etch temperature T, ΔE is the activation energy and K indicates the Boltzmann constant, 1.38×10^{-23} m^2 kg s^{-2} K^{-1}. Substitute v_s in Eq.2 by Eq.1, we have

$$\ln v_D = -\frac{\Delta E}{K}\frac{1}{T} + \ln\frac{A}{1+\tan\gamma\cot\theta} \quad (3)$$

Now we give out the distances of the edges with respect to the gravity centre of the etch pits developed in 300℃ and 310 ℃ KOH molten as shown in Fig10 (the etch pit morphologies for 300℃ and 310 ℃ are shown in Fig.A1 and Fig.A2, respectively, see the appendix). The distances similarly bear linear relation with the etch duration and corresponding fitted travelling speeds are 6.98nm/min and 12.25nm/min, respectively for the etching at 300℃ and 310 ℃. On the basis of Eq.3, dots showing (T^{-1}, lnv_D) were plotted in Fig.11, illustrating they lie around a line expressed as lnv_D=-11627 T^{-1}-2.46 by fitting. Consequently, the activation energy of the etching could be obtained as 96.6KJ/mol, which implys the etching speed for our experiment is controlled by the chemical reaction between Al_2O_3 and KOH but not by the diffusion of the reactants or the reaction productes [14].

a)

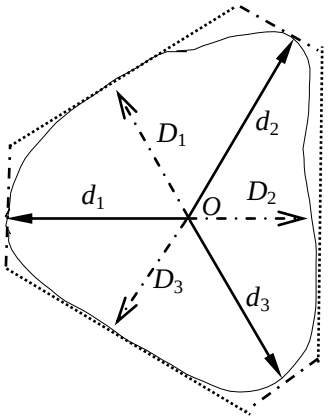

b)

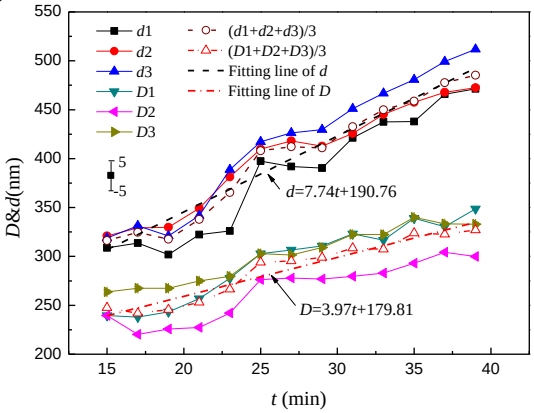

Figure 9 Distances of the edges with respect to the gravity centre O of the etch pit (etch temperature was 280℃).

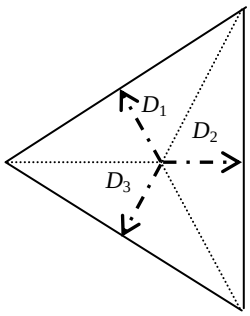

$$D = \frac{D_1 + D_2 + D_3}{3}$$

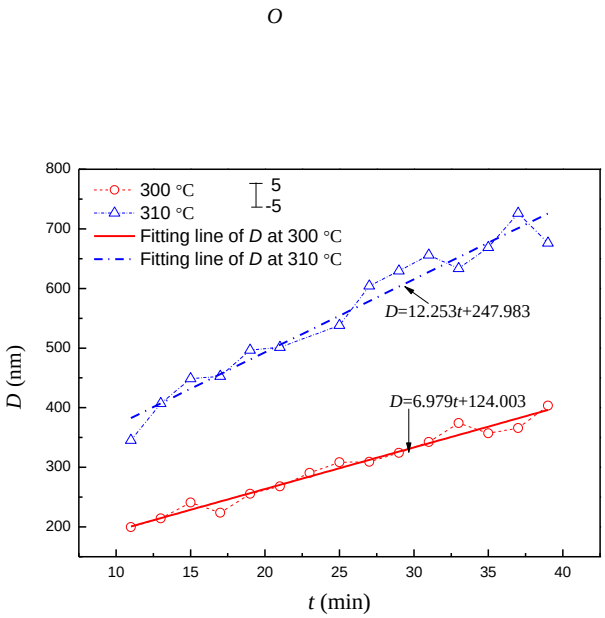

Figure 10 Distances of the edges with respect to the gravity centre *O* of the etch pits developed at 300℃ and 310℃.

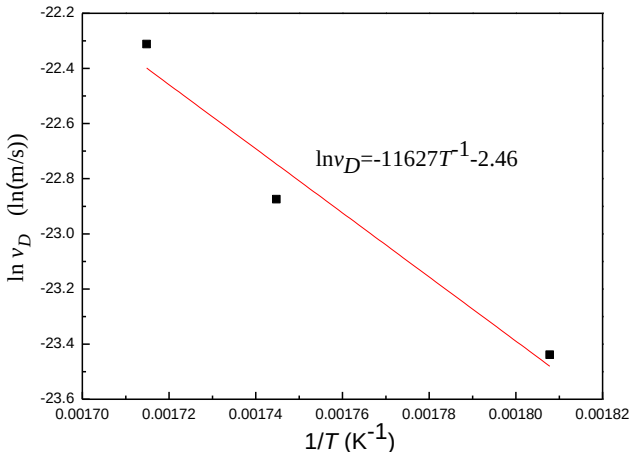

Figure 11 Fitting line showing relation of $\ln v_D$ and T^{-1}

4 Conclusions The present work experimentally studied the tridimensional morphology and kinetics of etch pit on the C-{0001} plane of sapphire crystal (α-Al_2O_3) in KOH molten. The results indicates that the tridimensional morphologies of etch pits on the {0001} plane of sapphire crystal show triangular symmetry consistent with the crystal symmetry of the sapphire, including regular triangular pyramid and hexagonal pyramid. They contain flat side walls belonging to the $\{1\bar{1}0\bar{2}\}$ family and $<11\bar{2}0>$ family edges on the etching surface. However, the triangular pyramid etch pit should be more stable than the hexagonal pyramid etch pit since the former full composed by Al^{3+} but the latter contains Al^{2+} on etching surface at atomic scale. As a result, the former would be observed with more possibility in practice.

Experiments shown that the etch pit developed during etching in manner of kinematic wave, which was, moreover, accomplished by the constant speed travelling of steps in fresh KOH molten. The travelling speed bear an Arrhenius formatted relation with the etch temperature, corresponding activation energy is 96.6KJ/mol, showing the etching is controlled by the chemical reation of Al_2O_3 and KOH.

References

[1] J. Xiao, S. Yin, M. Shao, and X. Zhang, Journal of Crystal Growth **266**,519-522 (2004).
[2] E.R. Dobrovinskaya, L.A. Lytvynov, and V. Pishchik, in: Sapphire: Material, Manufacturing, Applications, edited by, Micro- and Opto-Electronic Materials, Structures, and Systems, (Springer US, 2009), chap 1.
[3] C.M. Liu, J.C. Chen, Y.C. Huang, and H.L. Hsieh, Journal of Physics and Chemistry of Solids **69**,572-575 (2008).
[4] A.P. Honess, Pennsylvania State College, M . I. Exp.Sto.Bull. **3**,1-14 (1929).
[5] K. Sangwal, Crystalline Materials: Growth and Characterization, Series A, Key engineering materials **58**,187-204 (1991).
[6] E.R. Dobrovinskaya, L.A. Lytvynov, and V. Pishchik, in: Sapphire : Material, Manufacturing, Applications edited by, (Springer US, 2009), chap 2.
[7] J.A. Champion, and M.A. Clemence, Journal of Materials Science **2**,153-159 (1967).
[8] Robert Scheuplein, and Peter Gibbs, Journal of the American Ceramic Society **43**,458-472 (1960).
[9] W.J. Alford, and D.L. Stephens, Journal of the American Ceramic Society **46**,193-194 (1963).
[10]R.G. Vardiman, Journal of The Electrochemical Society **118**,1804-1809 (1971).
[11]J. Han, S. Meng, H. Zuo, and M. Zhang, China, CN200510010116.4. (2006).
[12]C. Motzer, and M. Reichling, journal of Applied Physics **108**,113523-113527 (2010).
[13]S. Amelinckx, The direct observation of dislocations, (New York, Academic Press, 1964).
[14]K. Sangwal, Etching of Crystals: Theory, Experiment, and Application, (Elservices North Holland, 1987).
[15]M. Szurgot, Crystal Research and Technology **25**,71-79 (1990).
[16]J.B. Bilde-Sørensen, B.F. Lawlor, T. Geipel, P. Pirouz, A.H. Heuer, and K.P.D. Lagerlo¨F, Acta Materialia **44**,2145-2152 (1996).
[17]http://icsd.ill.eu/icsd/deta ils.php?id[]=72131.
[18]G.J. Dienes, D.O. Welch, C.R. Fischer, R.D. Hatcher, O. Lazareth, and M. Samberg, Physical Review B **11**,3060 (1975).

[19]S. Blonski, and S.H. Garofalini, Surface Science **295**,263-274 (1993).
[20]P.D.S. Claire, K.C. Hass, W.F. Schneider, and W.L. Hase, J. Chem. Phys. **106**,7331-7342 (1997).
[21]I. Frank, J. Chem. Phys. **104**,8143 (1996).
[22]P. Hartman, and W.G. Perdok, Acta Crist. **8**,49–52, 521–524, 525–529 (1955).
[23]T. Li, K. Park, and K.R. Morris, Crystal Growth & Design **2**,177-184 (2002).
[24]J.M. Wittbrodt, W.L. Hase, and H.B. Schlegel, The Journal of Physical Chemistry B **102**,6539-6548 (1998).
[25]W. Schaarwächter, Physica Status Solidi (B) **2**,865-876 (1965).
[26]K. Sangwal, Journal of Materials Science **17**,2227-2238 (1982).

Appendix

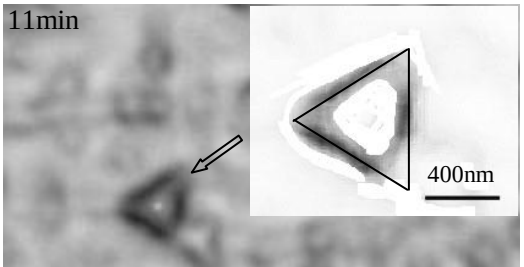

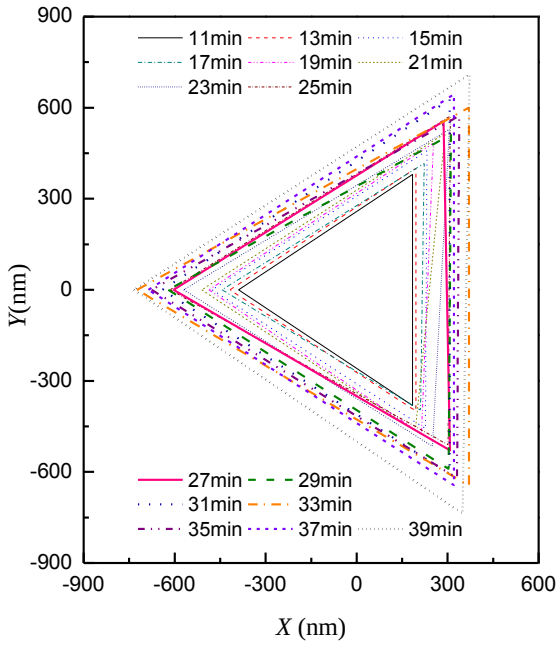

Figure A1 Etch pit morphologies in 300℃ KOH molten after different etch durations

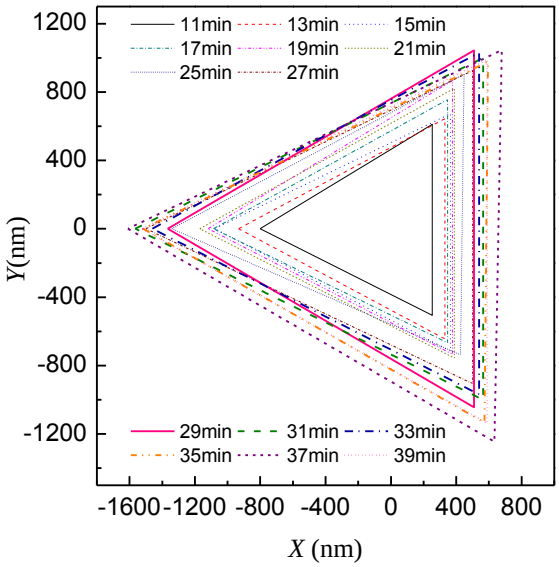

Figure A2 Etch pit morphologies in 310℃ KOH molten after different etch durations